QCD and QED dynamics of the EMC effect

Leonid Frankfurt,
School of Physics and Astronomy, Tel Aviv University, 69978 Tel Aviv, Israel

Mark Strikman
Penn State University, University Park, PA, 16802, U.S.A.

Abstract

Applying exact QCD sum rules for the baryon charge and energy-momentum we demonstrate that if nucleons are the only degrees of freedom of nuclear wave function , the structure function of a nucleus would be the additive sum of the nucleon distributions at the same Bjorken $x = AQ^2/2(p_A \cdot q) \leq 0.5$ up to very small Fermi motion corrections if $1/2m_N x$ is significantly less than the nucleus radius. Thus observations at CERN, SLAC, and TJNAF of the deviation of the ratio $R_A(x,Q^2) = (2/A)F_{2A}(x,Q^2)/F_{2D}(x,Q^2)$ from one reveal the presence of non-nucleonic degrees of freedom in nuclei. Employing the parton model (the QCD evolution equation) or exact QCD sum rules shows that the ratio $R_A(x_p,Q^2)$ used in experimental studies, where $x_p = Q^2/2q_0m_p$ deviates from one even if a nucleus consists of nucleons with small momenta only. Use of the Bjorken x in the theoretical analysis of experimental data leads in the case of the light nuclei to additional decrease of $R_A(x,Q^2)$ as compared to the plots presented in the experimental papers. Coherent contribution of Fermi, Weizsacker, Williams equivalent photons into photon component of parton wave function of a nucleus unambiguously follows from Lorentz transformation of the rest frame nucleus Coulomb field. Account of light cone fraction of nucleus momentum carried by equivalent photons almost compensates the difference between data analysis in terms of Bjorken x and x_p for heavy nuclei. Q^2 dependence of the hadronic EMC effect emphases difference of the interplay of the leading twist and higher twist effects for Q^2 probed at TJNAF and SLAC energies and those probed at CERN. Direct observations of large and predominantly nucleonic short-range correlations (SRC) in nuclei pose a serious challenge for most of the proposed models of the EMC effect for $x \geq 0.6$. The data are consistent with a scenario in which the hadronic EMC effect reflects fluctuations of inter nucleon interaction due to fluctuations of color distribution in the interacting nucleons. The dynamic realization of this scenario is presented in which quantum fluctuations of the nucleon wave function with $x \geq 0.5$ parton have a weaker interaction with nearby nucleons, leading to suppression of such configurations in bound nucleons and to the significant suppression of nucleon Fermi motion effects at $x \geq 0.55$ giving a right magnitude of the EMC effect. The directions for the future studies and challenging questions are outlined.

1 Introduction

Nearly thirty years ago the first observation of a difference between the nucleon and nucleus parton distributions was reported by the European Muon Collaboration (EMC) [1]. Hence such a difference is referred to as the EMC effect. The EMC measurement was followed by a series of experiments in the eighties which provided first information on the A-dependence of the EMC effect [2] and the A-dependence of antiquark distributions [3]. For a review of the data collected during the first decade of studies of the nuclear parton distributions see [4]. Interest in the EMC effect was revitalized by the recent high precision measurements at TJNAF for a range of the lightest nuclei [5]. To extract the EMC effect from experimental data one should account properly for the QCD dynamics of hard processes and the QED physics of equivalent photons accounting for electric charge of nucleus.

The parallel development is the BNL and TJNAF experimental studies which allowed one to observe directly the short-range correlations (SRC) in nuclei and explore their structure, for a review see [6, 7]. When combined with other experimental measurement of hard nuclear phenomena these observations put very strong constraints on the interpretation of the origin of the EMC effect which are not satisfied by many of the proposed explanations of the effect.

Another challenge for the models of the EMC effect based on the ideas taken from low energy nuclear physics are the data on antiquark distribution within a nucleon, nucleus.

In the review we restrict our discussion to the region $x \geq 0.2$ where nuclear shadowing (anti shadowing) phenomena are not important. For the recent review of small x leading twist physics and extensive list of references see [8].

Within the leading twist approximation of QCD nuclear structure functions depend on the Bjorken variable $x = AQ^2/2(q \cdot p_A)$ and Q^2 as the direct consequence of the dominance of hard interaction with a single parton in the leading twist hard processes. Description of structure functions in terms of the Bjorken variable x and Q^2 accounts for the renormalizability of QCD and QED. Account of Bjorken x i.e. the QCD dynamics removes artificial effect introduced by the EM collaboration and followed by all other experimental groups who ignored parton structure of wave function of nuclear target by using non-partonic variable $x_p = Q^2/2q_0m_p$ to compare nucleus and deuteron structure functions, see Figs. 1 and 2. Note that account of this effect leads to certain decrease of structure function of a nucleus i.e. sign of this effect is opposite to the one claimed in [9].

In the case of medium and heavy nuclei an additional effect becomes important: a nucleus at rest has an electric charge Z and related Coulomb field which is the zero component of electromagnetic field. Under the Lorentz transformation to the frame where the nucleus has a large momentum, the nucleus Coulomb field is transformed into the field of equivalent photons. This phenomenon is well known as the Fermi-Weizsacker-Williams (FWW) approximation [10]. Equivalent photons carry a noticeable and calculable fraction of the nucleus momentum if the parameter characterizing QED phenomena $Z\alpha_{em}$ is not too small. We evaluate this fraction which is dominated by the coherent contribution into

photon distribution in a heavy nuclear target [9].

Incoherent contribution into photon component of nucleus wave function is not negligible but it produces practically the same effects in the nucleus and nucleon distributions. So corrections to the additivity of nucleon structure functions due to incoherent photon component are tiny: $\approx (Z/A)\alpha_{em}$ multiplied by the probability of admixture of non-nucleon degrees of freedom in the nucleus wave function. The coherent photon distribution in protons and neutrons was evaluated previously in [11, 12], while in [13] the Q^2 evolution of incoherent photon distribution within a nucleon resulting from the Q^2 evolution of quark, antiquark nucleon parton distribution functions (pdfs) has been calculated [1]. However the implications of photon parton component for the momentum sum rule – one of the important phenomena in the case of medium and heavy nucleus – was considered only in [9].

Discussed above experimental and theoretical observations gives us a clue to the physics relevant for superdense nuclear matter - 3–5 nuclear densities (inner core of neutron stars, etc.) Really the BNL and TJNAF data show that short range nucleon correlations (SRC) in nuclei are dominated by the nucleon degrees of freedom; lack of nuclear effects in the antiquark distribution of nuclei shows that meson fields of bound and free nucleons are close at least up to the densities characteristic for SRC i.e. $\sim$ 3–5 average nuclear densities. Electromagnetic radius of bound and free nucleons are close. All these observations support validity of the equation of state suggested by the text book nuclear theory and therefore consistent with the recent observation of neutron stars with the mass around two solar masses. More generally these facts indicate that transition from low scale dynamics successfully described by effective Chiral QCD Lagrangian ($\Lambda_\chi \sim 1GeV$) to dynamics at higher resolution scale should be pretty intricate to be consistent with data on antiquark distribution within nucleons and nuclei.

The review is organized as following. In section 2 we explain why and how an account of the QCD dynamics allows us to fix dynamic variables eliminating kinematical effects introduced in the experimental studies which lead to the artificial breakdown of the nucleon additivity for the nuclear structure functions in the approximation when the nucleus is built of nucleons only.

In section 3 we build and analyze standard nonrelativistic nuclear physics approach where internal nucleon motion and the c.m. motion of the nucleus are independent. Within this approach a nucleus in the infinite momentum frame (or light-cone) consists of nucleons only. We use the exact QCD baryon number and momentum sum rules to derive the formula for the nuclear pdfs which takes into account nucleon Fermi motion and show that corrections to the ratio of nuclear structure functions due to this effect are small for $x \leq 0.55(0.7)$ for $F_{2N}(x,Q^2) \propto (1-x)^3 (\propto (1-x)^2)$. Hence it will be convenient in our theoretical discussion to consider separately two kinematical regions: $x \leq 0.5$ where

[1] Authors did not explicitly considered the total momentum fraction, though they calculated the photon parton distributions for all x.

the answer is expressed through the average deformation of the structure functions of the bound nucleon and $x \geq 0.6$ where interplay of quantum fluctuations of nucleon properties with the nucleon Fermi motion effects and SRC sets in.

In section 4 we evaluate the contribution of the simplest non-nucleonic component of nuclear structure functions - the photon structure function of a nucleus, $P_A(x, Q^2)$, calculate the fraction of the nucleus momentum carried by equivalent photons and extend the standard nuclear model to include this effect. This is feasible since coherent effects which give the dominant contribution in this calculation are model independent.

In section 5 we consider interplay of two model independent effects discussed in sections 3 and 4. EM collaboration introduced artificial correction to the ratio of nuclear and nucleon structure functions by comparing structure functions at x variable which differ from conventional Bjorken variable x required by QCD dynamics. Removing this correction leads to the increase of the EMC effect by about 20% for ^{4}He and a factor of two smaller for heavy nuclei (the absolute correction is about the same for ^{4}He while the EMC effect grows with A). At the same time the Coulomb effect discussed in section 4 generates a EMC like effect of comparable strength for $A \sim 200$ but opposite sign. As a result the hadronic component of the EMC effect is well described by the EMC ratio for heavy nuclei but underestimated for light and medium nuclei. The remaining effect represents the genuine "hadronic" EMC ratio which should be compared with the expectation of the Fermi motion contribution. One observes that deviation from the Fermi motion does not exceed 5% for $x \sim 0.5$ and much smaller for smaller x, indicating that wave functions of bound and free nucleon are very close for most of the quark-gluon configurations even at the central nuclear densities.

In section 6 we summarize the recent direct observations of the short-range correlations in nuclei which indicate that probability of such correlations is large (on the scale of 20%) and that nucleons in the SRCs are rather weakly deformed.

In section 7 we discuss interrelation between SRC and EMC effect and demonstrate that the A-dependence of the hadronic component of the EMC effect is consistent with the A-dependence of the SRCs.

In section 8 we summarize the most important constraints on the models of the EMC effect coming from the experimental studies of hard phenomena with nuclei and explain that wide classes of the current models are not consistent at least with one of these constraints.

In section 9 we consider plausible interrelation between well established properties of hard processes off a free nucleon and dynamics of the hadronic EMC effect. We explain that the observed rapid decrease of antiquark distribution within a nucleon at $x \geq 0.4$ indicates the suppression of meson field of a bound nucleon participating in hard processes. We argue that this suppression leads to a significant suppression of the contribution of SRC in the hard processes which select certain quark-gluon configuration in an interactive nucleon.Therefore Fermi motion effects and hence nuclear pdfs at $x \geq 0.6$ are suppressed as compared to the standard nuclear theory giving a right magnitude of the hadronic EMC effect at large x.

In section 10 we discuss briefly implications of discussed in the review effects on global fits of pdfs.

In section 11 we present the conclusions and implications of the EMC effect related physics for different phenomena.

2 Account of the QCD dynamics fixes the kinematic breakdown of the nucleon additivity for nuclear pdfs

It was proved long ago that in the limit $Q^2 \to \infty$, where Q^2 is the square of four-momentum transferred by electrons to the target, T, but fixed Bjorken x_T, the fraction of nucleus momentum carried by interacting parton:

$$x_T = Q^2/2(q \cdot p_T), \tag{1}$$

the structure functions of any target T are given by the convolution of cross section for hard probe scattering off individual patrons with parton distribution within this target:

$$\sum_n \int \psi_n^2(x_i, Q_0^2) \prod (dx_i) \delta(1 - \sum x_i) \delta(x_T - x_i). \tag{2}$$

The Bjorken scaling for the structure functions and Q^2 evolution follow from the asymptotic freedom in QCD and is implemented within the parton model accounting for the Q^2 evolution, the light-cone quantization of QCD and the Wilson operator product expansion. Normalization of the light-cone wave function (WF) of a target is derived based on the evaluation of the matrix elements of the exactly conserved currents between the WFs of the target in initial and final states at the zero momentum transfer (electromagnetic current, charmed, bottom currents). The parton model generalized to include the Q^2 evolution is the basis for QCD physics of hard processes, for the searches of new particles, etc.

Thus the appropriate variables to describe the process $e+A \to e'+X$ in terms of nuclear pdfs are the Bjorken variable x_A ($\equiv x_T$) and Q^2. To simplify formulae it is convenient to rescale Bjorken x_A by the factor A:

$$x/A = Q^2/(2q \cdot p_A). \tag{3}$$

So x/A is the fraction of the total nucleus momentum carried by the interacting parton and $0 < x/A < 1$. To investigate nuclear effects which can be interpreted within QCD the EM Collaboration introduced the ratio:

$$R_A = (2/A) F_{2A}(x, Q^2)/F_{2D}(x, Q^2). \tag{4}$$

It is important to realize that the EMC ratio as defined in Eq.4 is presented in the experimental papers as a function of the variable $x_p = Q^2/2q_0 m_p$ [1] (also it was normalized

to the cross section of electron – deuteron scattering rather than to the sum of the electron – proton and electron–neutron cross sections). Such variable is convenient for experimental studies as one can compare the cross sections of the lepton - nucleus scattering for the same kinematics of the incident and final lepton. Variable x_p differs from the parton model variable x and therefore within the parametrizations of structure functions in terms of x_p Bjorken scaling and well established universality of hard processes obtain unconventional form which is in variance with the physical intuition. In particular, the ratio $R_A(x_p, Q^2)$ defined similar to Eq. 5 is different from one in the kinematics where γ^* scatters off bound nucleon carrying $x_A = 1/A$ fraction of nucleus momentum, i.e. off a bound nucleon at rest in the nucleus target rest frame. Thus the baryon charge and momentum sum rule are violated within a model where nucleus consists of nucleons only etc. Moreover nuclear pdfs presented as a function of x_p cannot be used directly without the additional correcting factor to predict hard phenomena in pA and AA collisions where as the consequence of the QCD factorization theorem the hard cross sections are controlled by the parton distributions over the Bjorken x fraction of the colliding nucleus energy carried by the interacting parton.

We will demonstrate in the next section that the use of the Bjorken x instead of x_p leads to a 20% enhancement of the EMC effect for the lightest nuclei ($A \leq 12$) for $x \sim 0.5$ and to somewhat smaller correction for heavy nuclei. We correct here mistake made in [9] in the process of restoring Bjorken scaling and QCD evolution violated in experimental studies, see also [14] and Fig.1 below. For medium and heavy nuclei a comparable contribution to the EMC ratio but of opposite sign originates from another model independent effect - presence of the equivalent photon field of nuclei (section 4).

3 Standard model for the structure functions of nuclei

In order to discuss to what extent the EMC effect signals presence of new physics in the nuclear structure we need to establish expectations of the textbook nonrelativistic nuclear model in which nuclei are build only of nucleons which have the same internal structure as free nucleons. We will refer to this approximation as the standard nuclear model. (Actually the standard model should be extended to include also equivalent photons as non-nucleonic degrees of freedom. This will be done in the next section.)

At the first step of our analysis the Fermi motion of nucleons can be neglected. Let us consider a nucleus moving with a large momentum P and a parton which carries a fraction x_A of the nucleus momentum. Each nucleon carries fraction P/A of the nucleus momentum since the Fermi motion of the nucleons is neglected. Hence this parton carries a fraction Ax_A of the nucleon momentum. As a result we find

$$f_A^j(x_A, Q^2) = Z f_p^j(Ax_A, Q^2) + N f_n^j(Ax_A, Q^2), \tag{5}$$

where $x_A = Q^2/2(q \cdot P)$. In the case of deep inelastic scattering necessity to use x_A follows from the fundamental property of parton model that γ^* interacts with an individual parton.

Note that the exact QCD sum rules for the baryon charge and momentum conservation were derived using Eq.5 or by direct calculation of matrix elements of conserved currents: the baryon charge and the energy-momentum tensor. Since in this approximation f_A^j is equal zero for $x_A \geq 1/A$ it is convenient to rescale

$$x_A \to A x_A = x, \tag{6}$$

so that x is now changing between 0 and A and consider the ratio

$$R_A^j(x,Q^2) = \frac{f_A^j(x,Q^2)}{Z f_p^j(x,Q^2) + N f_n^j(x,Q^2)}. \tag{7}$$

If there are no nuclear effects,

$$R_A^j(x,Q^2) = 1. \tag{8}$$

In the nonrelativistic approximation to the nucleon Fermi motion, the nucleus c.m. motion is separated from the inner motion of nucleons. So the light- cone WF of a nucleus, $\psi_A = \exp i(\vec{p}_A \cdot \vec{x})\psi_{int}$, can be conveniently calculated in terms of equal time WF of the nonrelativistic nuclear theory - ψ_{int}. Here p_A is nucleus momentum and $\vec{x}$ the coordinate of the nucleus center of mass. Thus the Lorentz boost in this approximation is trivial – it is reduced to the transformation of the plane wave. This property allows us to use the experience of the low energy nuclear physics to evaluate some hard QCD phenomena.

There exists a variety of the exact sum rules for valence quark distribution which follow from the Ward identities and existence of exactly conserved currents: baryon charge, isotopic charge etc. The typical valence quark sum rule for the baryon charge and the momentum sum rule are:

$$\int_0^A dx V_A(x,Q^2) = B, \tag{9}$$

$$\int_0^A dx [x V_A(x,Q^2) + x S_A(x,Q^2) + x G_A(x,Q^2)] = A. \tag{10}$$

Here $xV_A(x,Q^2)$ is the density of valence quark distribution, $x_A S_A(x_A,Q^2)$ is the density of nucleus sea quark distribution, $xG_A(x,Q^2)$ is the density of nucleus gluon distribution. B is nucleus baryon charge. An additional factor of A in Eq. 10 reflects our choice of scale for x – the fast momentum is measured in units of p_A/A that is average nucleon momentum (in the model where nucleus is build only of nucleons in the fast frame).

In this section we consider nucleus as a system of nucleons and use the above sum rules to derive approximate formulae for the nuclear pdfs accounting for relativistic corrections due to nucleon Fermi motion. In the impulse approximation nuclear pdfs are described by the convolution formulae :

$$f_A^j(x,Q^2) = \int_x^A \frac{d\alpha}{\alpha} \left[f_p^j(x/\alpha,Q^2)\rho_A^p(\alpha) + f_n^j(x/\alpha,Q^2)\rho_A^n(\alpha) \right]. \tag{11}$$

Here $\rho_A^{p,n}(\alpha)$ is the proton (neutron) light-cone densities of the nucleus, α/A is the fraction of nucleus momentum carried by interacting nucleon, Z and N are the numbers of protons and neutrons. The evaluation of the matrix element of the conserved currents (electromagnetic, isotopic, baryon charge) – $\langle A|\, J_\mu(t)\, |A\rangle$ at the zero momentum transfer, t between nucleus states gives [15]:

$$\int_0^A \rho_A^{p,n}(\alpha)\frac{d\alpha}{\alpha} = Z(N). \tag{12}$$

Evaluation of the matrix element of the energy-momentum tensor gives [15]:

$$\int_0^A \frac{1}{A}[\rho_A^p(\alpha) + \rho_A^n(\alpha)]d\alpha = 1. \tag{13}$$

Since the nucleus is a nonrelativistic system, the light-cone density is concentrated near $\alpha = 1$. Hence it is legitimate to evaluate the contribution of the Fermi motion for $x < 0.7$ by decomposing integrand of Eq.11 in the Taylor series in powers of $\alpha - 1$ and account for the first three terms in the expansion. Thus the contribution of the Fermi motion effect to the ratio defined in Eq. 7 is [15, 16]:

$$\begin{aligned} R_A(x,Q^2) = \frac{1}{A}\int_0^A \rho_A^N(\alpha)\frac{d\alpha}{\alpha} + \frac{x{f_j}^{N\prime}(x,Q^2)}{f_j^N(x,Q^2)}\left[1 - \int_0^A \rho_A^N(\alpha)d\alpha/A\right] \\ + \frac{x f_j^{N\prime}(x,Q^2) + \frac{x^2}{2} f_j^{N\prime\prime}(x,Q^2)}{f_j^N(x,Q^2)}\frac{1}{A}\int_0^A \rho_A^N(\alpha)(1-\alpha)^2\frac{d\alpha}{\alpha}. \end{aligned} \tag{14}$$

Here $f_j^N = (f_j^p + f_j^n)/2$ and we assumed equal number of protons and neutrons. In the first term in the above equations the nucleon structure functions are cancelled in the ratio since the variable x is independent of the atomic number the resulting factor is equal to one due to the normalization condition Eq.12.

It is worth emphasizing that the discussed decomposition becomes inapplicable at large x since it diverges for $x \sim 1$. In this region $R_A(x,Q^2)/R_{A'}(x,Q^2) \sim \langle T_A\rangle/\langle T_{A'}\rangle$ which is qualitatively different from Eq.14. Here $\langle T_A\rangle$ is the average kinetic energy.

It is convenient to introduce

$$\eta_A = 1 - \int_0^A \rho_A^N(\alpha)d\alpha/A \equiv \langle 1-\alpha\rangle\,, \tag{15}$$

the fraction of the light-cone momentum which is carried by nuclear constituents other than nucleons. It is equal to zero if nucleus consists of nucleons only , but we keep this term in anticipation of the discussion of the effect of equivalent photons below. In the nonrelativistic limit $k^2/m_N^2, \epsilon_A/m_N \ll 1$ (ϵ_A is the nuclear binding energy per nucleon) the nuclear factor in the third term of Eq.14 $\langle(\alpha-1)^2\rangle = A^{-1}\int_0^A \rho_A^N(\alpha)(1-\alpha)^2\frac{d\alpha}{\alpha}$ can be calculated using nonrelativistic approximation for $\alpha \approx 1 + k_3/m_N$ where k is nucleon

three momentum within the nucleus target. (The formula $\alpha \approx 1 + k_3/m_N + O(k^2/m_N^2)$ This leads to

$$\langle(\alpha-1)^2\rangle = \frac{k^2}{3m_N^2} + O(k^4/m_N^4, \epsilon_A^2/m_N^2) = \frac{2T_A}{3m_N}. \tag{16}$$

This allows us to rewrite Eq. 14 as

$$R_A(x,Q^2) = 1 + \frac{x{f_j}^{N\prime}(x,Q^2)}{f_j^N(x,Q^2)}\eta_A + \frac{x{f_j}^{N\prime}(x,Q^2) + \frac{x^2}{2}{f_j}^{N\prime\prime}(x,Q^2)}{f_j^N(x,Q^2)}\frac{2T_A}{3m_N}. \tag{17}$$

In the case of $f_N^j(x,Q^2) \propto (1-x)^n$, Eq. 17 can be written as

$$R_A(x,Q^2) = 1 + \frac{nx(x(n+1)-2)}{(1-x)^2}\cdot\frac{T_A}{3m_N} - \eta_A nx/(1-x). \tag{18}$$

We will present numerical results in section 5. Here we just note that it follows from Eq.18 that for $x \leq 0.5$ ($x \leq 0.7$) for n=3(n=2) effects of Fermi motion are small and under control as the consequence of the account for the exact conservation laws. The Fermi motion gives zero contribution to R_A at $x = 2/(n+1)$, a small negative contribution at $x < 2/(n+1)$ and leads to a rapid growth of R_A at $x > 2/(n+1)$. In this discussion we ignored Q^2 dependence of structure functions. We will show in the end of this section that higher twist (HT) effects play significant role at ≥ 0.5 and $Q^2 \sim$ few GeV^2.

At the same time the experimental data on nuclear pdfs are usually presented in terms of the variable

$$x_p = Q^2/(2m_p q_0), \tag{19}$$

which is different from the fraction of target momentum carried by interacting parton and therefore requires rewriting formulae for parton model and Q^2 evolution. This variable depends on the atomic number of a target even if the nucleon Fermi motion effects are neglected.

$$x_p/x = m_A/Am_p = (1 - (\epsilon_A - (m_n - m_p)N/A)/m_p) \equiv 1 + r_x. \tag{20}$$

Thus the structure functions of interacting nucleons in the nominator and denominator depend on different arguments [2] Thus the use of variable x_p instead of x (and the expectation of absence of the nuclear effects in such an approximation) violates important condition of standard nuclear model that nuclear pdfs are the sum of nucleon pdfs if the Fermi motion effects are neglected and introduces artificial dependence of R_A on atomic number. In particular $R_A(x) = 1$ corresponds to

$$R(x_p) = f_A^j(x(1+r_x))/f_N^j(x) \approx 1 - r_x n\frac{x}{1-x}, \tag{21}$$

[2] In ref. [9] and in the original version of this paper a mistake in the sign of r_x was made which resulted in a wrong sign of the discussed effect.

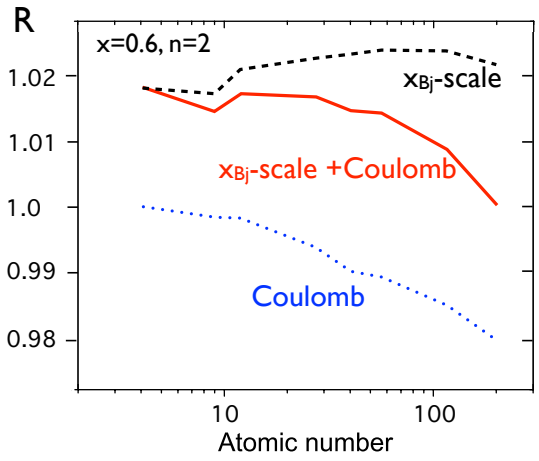

Figure 1: Change of R due to account for correct x-scale(dashed line), contribution of equivalent photons (dotted line) and combined effect (solid line) as a function of atomic number for $x = 0.6$ and $F_{2N}(x) \propto (1-x)^2$.

where at the last step we took $f_N^j(x) \propto (1-x)^n$ [3]. The value of the correction to the EMC effect due to this effect is presented in Fig.1 together with the effect of equivalent photons to be discussed in the next section and combined effect which reflects the change of the hadronic component of the EMC effect.

The nucleon Fermi motion correction can be easily included as well. We will demonstrate in section 5 that Eq.21 leads to decrease of R_A, enhancing the EMC effect for $A \geq 4$ by practically the same amount due to a weak A-dependence of x_p for $A \geq 4$. We will explain in the next section that for heavy nuclei presence of the Coulomb field for a nucleus at rest explains a certain fraction of the EMC effect which compensates the effect of change of x_p. So the hadronic contribution to the EMC ratio for heavy nuclei is close to the EMC ratio reported experimentally. Overall account of the two effects leads to reduction of the A-dependence of the hadronic contribution to the EMC ratio for A between 4 and 200, cf. Fig. 5.

Comment. A popular expectation in the low energy nuclear physics is that one can account for the effects of relativistic nucleon Fermi motion assuming that the vertex functions in the Feynman diagrams with a virtual nucleon coincide with Schrodinger WFs of a nucleus. This model has been applied in several papers to explain the EMC effect formulated in terms of non-parton model variable x_p and without subtraction of the contribution of equivalent photons. In the first papers [17, 18] the baryon sum rule, i.e., the

[3]Note that to simplify the expressions we took here $m_n = m_p$ so the dominator x consider with x_p. In the final expressions the A/D ratio we will take into account the difference between x_p and x_D.

probability conservation was violated. Later the baryon charge sum rule has been taken into account following the prescription of [19]. This description does not allow one to account consistently for the probability conservation i.e. to satisfy simultaneously both baryon and momentum sum rules for the hadronic part of the EMC effect. Thus within this approach light-cone nucleus wave function contains non-nucleonic degrees of freedom. They are hidden in the internucleon interaction and identified in the text books of nuclear physics with meson exchanges. Such hypothesis has problem to explain the observation of no nuclear effects in the antiquark distribution in nuclei.

The baryon sum rule in this model is derived by calculating matrix element of baryon charge exactly. The calculation leads to the normalization of the nucleus wave functions in terms of the value of nucleus baryon charge. This unambiguous normalization differs from the nonrelativistic normalization of the nucleus WF. [4] (Note that normalization of wave function natural for the nonrelativistic physics implies correction to the total cross section of DIS off deuteron of the same magnitude as the Glauber shadowing correction which violates probability conservation – the so called West correction[20]). In this approach there is no symmetry between distributions over fractions of nucleus momentum carried by interacting nucleon and nucleon spectators. As a result in this model significant light-cone fraction of the nucleus momentum is carried by the non-nucleonic degrees of freedom [16]:

$$\eta_A = \epsilon_A/m_N + T_A/3m_N, \tag{22}$$

Here ϵ is the nucleus energy binding per nucleon. T_A is the average kinetic energy of a bound nucleon, For the realistic nuclear WFs and $A \geq 40$, Eq. 22 leads to $\eta_A \sim 2\%$ which corresponds for the Jlab, SLAC kinematics where $n \sim 2$ to $R_A(0.6) \sim= 0.94$ which is about $1/2$ of the observed effect. So this approach when including the Bjorken definition of x and taking into account the contribution of equivalent photons has problems to describe observed dependence of R_A on x and absolute value of R_A.

3.1 Scaling violation and Fermi motion effects

The experimental data on $F_{2N}(x, Q^2)$ for large x indicate that the x-dependence of $F_{2N}(x, Q^2)$ changes strongly with Q^2. Usually this effect is interpreted as due to the presence of the higher twist effects for small W / low Q^2 which can be written in the form

$$F_{2N}(x, Q^2) = F_{2N}^{LT}(x, Q^2)(1 + \frac{c}{(1-x)Q^2} + 1 + \frac{d}{(1-x)^2Q^4}). \tag{23}$$

The fits to the SLAC and Jlab data corresponding to typical $Q^2 = 5$ GeV^2 give $F_{2N}(x, Q^2) \propto (1-x)^n, n = 2$ [21] while for the large x data taken at CERN typical $Q^2 = 40$ GeV^2 , $n \sim 3$ [22]. This increase of the effective n with Q^2 is consistent with the expectations of Eq. 23 that the HT effects should die out with increase of Q^2 for fixed x.

[4] For the detailed discussion of the early theoretical studies of these issues and references see [16].

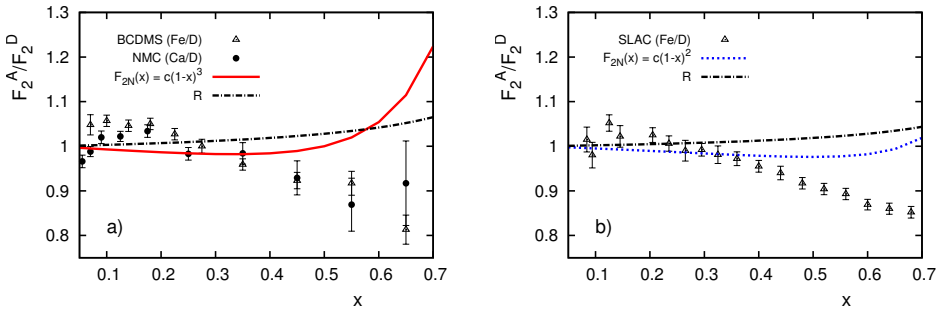

Figure 2: Effect of Fermi motion on the EMC ratio for large and moderate Q^2 - solid and dashed curves and the effect of f proper definition of x (with a small correction due to equivalent photons) - dot-sashed curved. The data are from [23] – right figure and from [24, 25] - left figure.

One can see from Eq. 18 that the Fermi motion effect is strongly modified when n changes from 2 to 3 , cf. Fig. 2. Also with increase of x average x/α in the convolution integral start to exceed significantly x leading to enhancement of the higher twist contribution to the EMC ratio. The correction due to the difference between x and x_p increases between low and high Q^2 by a factor of $\sim 3/2$. Similarly the effect of the extra degrees of freedom in Eq. 18 also changes by a factor of $\sim 3/2$.

Note in passing that there may exist specific nuclear HT effects. One example is the quasielastic contribution which becomes significant for moderate Q^2 for $x \geq 0.8$. Another potential source of the nuclear HT effects is scattering off the SRC where 6 quarks come rather close together.

4 Photon distribution in nucleons and nuclei.

4.1 General framework

The long range Coulomb field of nucleus at rest is the zero component of the electromagnetic field. Lorentz transformation of nucleus Coulomb field from rest frame to the frame where nucleus is rapid unambiguously leads to the field of Fermi, Weizsacker and Williams equivalent photons [10]. Thus the light-cone WF of nucleus contains photons as constituents carrying a fraction of the nucleus momentum. Collision of equivalent photons of one nucleus with nucleon or nucleus beams produces variety of hard and soft high energy processes in the ultraperipheral processes at the LHC [26]. Ultraperipheral processes were observed at RHIC, see review in [26].

For this paper a proper example of the ultraperipheral processes is the diffractive production of massive lepton pairs $\gamma^* + A \to L^+ + L^- + A$. Large Q^2 and/or large mass of

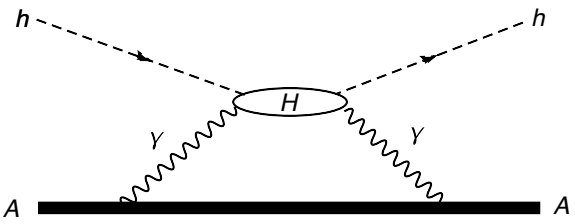

Figure 3: Diagram for the interaction of photon of the nucleus with a hard probe h.

the lepton pair L^+L^- guarantees dominance of the leading twist term and allows one to define photon distribution in a nucleus, $P_A(x,Q^2)$.

A nucleus is characterized by quark, gluon, photon distributions within a nucleus. To suppress particle production by hard probe from vacuum the gauge condition $A^+ = 0$ is chosen, where A_μ is the operator of photon field. In this gauge photon distribution has the form familiar from QED, cf. Fig. 3. The photon parton distribution can be written as the matrix element of the product of the operators cf. [27]:

$$P_A(x,Q^2) = \frac{1}{\pi}(2\pi x p^+)^{-1}\int_{-\infty}^{\infty} dy^- \exp\left(-i(x/A)p^+y^-\right) \cdot 1/2\sum_\mu \langle A\left|\left[F_\mu^+(0,y^-,0),F^{\mu,+}(0)\right]\right|A\rangle_{A^+=0}. \quad (24)$$

Here $F_{\mu,+}$ is the operator of the strengths of the photon field with transverse component μ, and $x/A = Q^2/2(p_A q)$ is the fraction of nucleus momentum carried by a parton.

To simplify calculations it is convenient to represent P_A as the sum of two contributions $P_A = P_A^{inel} + P_A^{coherent}$. First term accounts for the target excitations by virtual photon - we will refer to it as the inelastic term. The second term is the contribution of equivalent photons. We will refer to it as the coherent term.

Small value of α_{em} guarantees that in the kinematic domain achievable at accelerators $\alpha_{em}\ln(Q^2/\lambda^2_{QCD})/2\pi \ll 1$ and therefore all effects of this order can be neglected. In particular, in this kinematic domain the effects of running of $\alpha_{em}(Q^2)$ due to combined QED and QCD effects are negligible. Moreover it is legitimate to neglect in this kinematics by the Q^2 evolution of the amplitude of the scattering of a hard probe h off the photon which leads to tiny corrections. There are two practical consequences. The Q^2 evolution of inelastic photon distribution in a target T – $P_T(x,Q^2)$ goes in one direction: quarks, antiquarks radiate photons in the process of evolution but a photon does not radiate them. This evolution is accounted for in the evolution equation through the Q^2 dependence of valence, sea quark and gluon densities. At $1/2m_N R_A \le x \le 0.6$ where nuclear shadowing (anti shadowing) effects and nucleon short range correlations are a small correction, the account of inelastic photon distribution does not violate additivity and therefore does not change significantly R_A - (such an effect is suppressed since it is proportional to a product

of two small factors: the smallness of e.m.correction and the overall smallness of the EMC effect).

Second consequence of the smallness of the electromagnetic constant is that coherent contribution is not evolving with Q^2 at Q^2 achievable experimentally. Coherent contribution due to Z^2 dependence violates additivity and changes R_A .

Above we defined P_A^{inel} exactly in the same way as other parton densities, cf. Eq. 24. This definition allows to calculate P_A^{inel} in terms of quark, antiquark nuclear pdfs by evaluating corresponding Feynman diagrams.

$$xP_A^{inel}(x,Q^2)/A = \frac{\alpha_{e.m.}}{\pi}\int_0^{k^2_{tmax}} dk_t^2 \int_{\nu_{min}}^{\nu} \frac{d\nu'}{\nu'} \frac{k_t^2}{(k_t^2+Q^2\nu'/\nu)^2} F_{2A}(\nu',k_t^2)/A. \qquad (25)$$

Within the leading $\alpha_{e.m.}\log k_t^2$ approximation upper limit of integration over photon transverse momentum is ensured by the square of nuclear form factor . So $k^2_{tmax} \approx (3/r_A^2) \leq Q^2$. Since dominant contribution arises from small k_t sensitivity to nuclear form factor at essential x is weak. Here $\nu = 2(pq)/A = Q^2/x$, k_t is the transverse momentum of the photon, and $F_{2A}(\nu,Q^2)/A$ is the virtual Compton amplitude normalized per nucleon. In the above formulae we neglected the small contribution of the longitudinally polarized photons (F_L^A).

The presence of equivalent photons in the nuclear WF leads to the violation of the intuitive prediction we discussed in sections 2, 3 – $R_A^j(x,Q^2) = 1$, for $x \leq 0.5$:

$$R_A^j(x,Q^2) = \frac{Zf_p^j(x/(1-\eta_\gamma),Q^2) + Nf_n^j(x/(1-\eta_\gamma),Q^2)}{Zf_p^j(x,Q^2)+Nf_n^j(x,Q^2)}. \qquad (26)$$

Here $\eta_\gamma(A)$ is the fraction of nucleus momentum carried by equivalent photons calculated in [9]. Account of the presence of $\eta_\gamma(A)$ leads to a definite dependence of R_A^j on Z and A. For example this effect is as large as the effect of accounting for the difference between x and x_p for heavy nuclei but opposite sign while it is negligible for Z=2.

4.2 The coherent and incoherent contributions into photon distribution of a nucleus

First we will calculate coherent contribution to parton nucleus distribution which dominates the photon distribution in a nucleus. This contribution to $P_A(x,Q^2)$ arises from the interaction of a hard probe with a photon coherently emitted by the target so that the target remains intact, cf. Fig.3. The coherent contribution to the photon structure function is unambiguously calculable in terms of the electromagnetic form factors of the nucleus target. For a proton target coherent term has been calculated in [11]. Inelastic contribution for a nucleon target (where nucleon is excited in the final state) was calculated in the perturbative QCD model where quarks and gluons are generated via evolution starting at very small Q^2 [12]. Comparison of two contributions was performed at [13] where it was

found that the elastic contribution is much more important in the proton case in a wide range of the x, Q^2. In the neutron case incoherent contribution is more important.

An important aspect of the photon contribution – its implications for the momentum sum rule was not discussed in these papers and effects of the presence of photons in addition to quarks and gluons at the normalization scale are still not included in the pdf studies by the groups which analyze the hard processes. We calculate the field of equivalent photons through the evaluation of Feynman diagram in Fig.3. Calculations are simplified in our case since the nucleus is heavy so the static approximation should be sufficiently accurate. In the static approximation zero component of photon momentum in the nucleus rest frame is negligible: $k_0 = k^2/2m_A \approx 0$. So

$$x = A(k_0 - k_3)/M_A \approx -k_3/m_N. \tag{27}$$

Second simplification arises from the observation that four-vector k can be decomposed over directions defined by external momenta: $k_\mu = ap_\mu + bq_\mu + k_t$. Here p is four momentum of target nucleus and q is four momentum of virtual photon (external hard probe) and $(pk_t) = (qk_t) = 0$. In the essential region: $p_\mu A_{\mu,\lambda} \approx (k_{t\mu}/a)A_{\mu,\lambda}$, cf. [28]. Account of this property leads to the generalization of the Fermi - Weizsacker -Williams expression for the spectrum of the equivalent photons:

$$xP_A^{coherent}(x, Q^2) = \frac{\alpha_{em}}{\pi}\frac{Z^2}{A}\int dk_t^2 k_t^2 \frac{F_A^2(k_t^2 + x^2m_N^2)}{(k_t^2 + x^2m_N^2)^2}, \tag{28}$$

Here $F_A(t)$ is the observed electric form factor of the nucleus which is equal to the product of the nucleus body form factor and the proton electric form factor $F_p(t)$. Hence the characteristic values of k_t^2 are small.

In our estimates we choose F_A in the exponential form, i. e.

$$F_A(k_t^2 + x^2m_N^2) = \exp(-r_A^2(k_t^2 + x^2m_N^2)/6). \tag{29}$$

Here r_A is the experimentally measured RMS nuclear radius and m_N is the nucleon mass. Such a form allows one to perform the numerical integration over the transverse momenta of the photons.

It is useful to compare different electromagnetic contributions. The most important one is the contribution of equivalent photons in which the fields of individual protons add coherently. This coherence leads to a larger momentum fraction carried by the photon field in nuclei as compared to that carried by individual free protons. Eq. 28 can be used to evaluate the coherent contribution of the photons to the momentum sum rule (here we already subtracted contribution of individual protons to the photon parton density - see discussion below, since this quantity enters into description of the nuclear effects we discuss in the paper):

$$\eta_\gamma = \int_0^1 dx x P_A(x, Q^2) = \alpha_{em}\frac{2}{\sqrt{3\pi}}\frac{Z^2}{A}\frac{1}{m_N r_A}. \tag{30}$$

To separate nuclear effects one need to subtract the contribution of Coulomb fields of protons. This is achieved by taking into account contribution of the incoherent break up of the nucleus as well as production of hadrons (inelastic processes). Sum of the two effects can be calculated in the closure approximation where cross section is described by the sum of two diagrams presented in [29] and results in replacing $Z^2F_A^2(t) \longrightarrow ZF_N^2(t)+Z(Z-1)F_A^2(t)$ in Eq. 28 leading to

$$\eta_\gamma = \int_0^1 dx x P_A(x,Q^2) = \alpha_{em}\frac{2}{\sqrt{3\pi}}\frac{Z(Z-1)}{A}\frac{1}{m_N r_A} + \frac{Z}{A}\eta_p \tag{31}$$

The second term in Eq.31 is due to the Coulomb field of the individual protons and it is included in the structure functions of the proton. Hence it should not be included in the calculation of the nuclear effects. The contribution of magnetic form factors of neutron and proton is negligible because it is concentrated at larger momentum transfers than the scale of the nuclear phenomena.

Taking r_A from the compilation of ref.[30] we find for the nuclear term in Eq.31

$$\eta_\gamma(^4He) = .03\%; \eta_\gamma(^{12}C) = .11\%; \eta_\gamma(^{27}Al) = .21\%;$$
$$\eta_\gamma(^{56}Fe) = .35\%;\ \eta_\gamma(^{197}Au) = .65\%. \tag{32}$$

To evaluate the impact of the presence of the photon component for the nuclear structure functions we can use Eq.18 and take $\eta_A = \eta_\gamma(A)$. The small x nuclear shadowing effects modify this approximation, however they are negligible for $x \geq 0.2$ range we are interested in and give insignificant contribution into momentum sum rule. Since deviations from the additivity are small the effect of the presence of the photons and other "hadronic" effects can be treated as contributing additively to the deviation of the EMC ratio from one. Larger numbers given in [9] are because of misprint in the formulae for coherent contribution and due to inaccurate numerical calculation.

4.3 Equivalent photons and modification of the initial condition for the Q^2 evolution of nucleus and nucleon pdfs

Major impact of the presence of the photon constituents in a nucleus is through the change of the form of the energy-momentum conservation and violation of isotopic invariance in the incoherent contribution of protons and neutrons. Total fraction of nucleus momentum carried by QCD partons instead of 1 becomes: $1-\eta_\gamma(A)$ (in this fraction the photon fields due to individual nucleons are included).

The presence of the photon component in the nuclear light-cone WF leads to the certain modification of Q^2 evolution of parton densities. Most important is the change of the momentum sum rule due to necessity to account for the fraction of nucleus momentum carried by photons:

$$\int_0^A \left[(1/A)(xV_A(x,Q^2) + xS_A(x,Q^2) + xG_A(x,Q^2))\right] dx =$$

$$1-\int_0^A \left[(1/A)xP_A(x,Q^2)\right]dx = 1-\eta_\gamma(A). \quad (33)$$

The light cone momentum carried by equivalent photons is compensated by the loss of the momentum by the nucleons. Since the nucleus Coulomb field is the collective field dominated by the contribution of large impact parameters, the reduction of the light cone fraction is experienced by nucleus as a whole (i.e. by both protons and neutrons.) Hence the shift is approximately equal for protons and neutrons.

Although $\eta_\gamma(A)$ is small its role is enhanced by the rapid decrease of nuclear pdfs with x increase.

In the case of a nucleon target one should also account for the change of the form of the momentum conservation and much larger contribution of photons for the proton target than for the neutron target leading to an isospin violating effect for pdfs of protons and neutrons and hence for the nuclear targets.

5 Implications for the EMC effect for nuclear pdfs at $x \leq 0.5$

Here we study to what extent two effects we discussed above - the proper definition of x which preserves the momentum sum rule, and the account of the collective Coulomb field of the nucleus (of the momentum carried by equivalent photons) - which we refer below as the standard model of the nucleus - explain the data at $x \leq 0.5$ where Fermi motion is a small correction.

In the standard model we can use Eqs. 18,21 to obtain

$$R_A^j(x_p) = f_A^j(x(1+r_x+\eta_\gamma))/f_N^j(x) = 1-(r_s+\eta_\gamma)n\frac{x}{1-x}+\frac{nx(x(n+1)-2)}{(1-x)^2}\cdot\frac{T_A}{3m_N}. \quad (34)$$

Since the EMC ratio is experimentally defined relative to the deuteron one needs to substitute $r_x(A)$ by $r_x(D)$. The results of calculations using Eq.34 with T_A from [31] are presented in Fig. 2 for medium A nuclei for low and high Q^2. We show separately the effect of Fermi motion and the combined effect of the account for the x-scale and for Coulomb effects.

One can see that the the Fermi motion effect is very different for low and high Q^2 especially for $x \geq 0.55$. [5].

Overall inspection of Fig.2 indicates that the contribution to EMC effect due to the modification of the quark distribution in nucleons is significant only for $x \geq 0.5$.

The effect of the correcting for the difference of x_p and x leads to an increase of the EMC effect which is very similar to all nuclei with $A \geq 4$ since the energy binding is a weak function of A. Effect is much smaller for the case of ^{3}He namely for the ratio $F_{2^3He}(x_p)/[F_{2\,^2H}(x_p)+F_{2p}(x_p)]$ due to a very small energy binding per nucleon in ^{3}He.

[5] The data for heavy nuclei [23] were corrected for the difference of the number of protons and neutrons.

Absolute value of the EMC effect for this ratio is rather uncertain since the magnitude of the effect is comparable to the normalization uncertainty [32]. However an effect on the level of 1/4 of the effect for heavy nuclei (the A-dependence expected from the contribution of the short-range correlations - see discussion below) - cannot be excluded.).

Overall the proper choice of the x-scale – that is the choice of Bjorken x – increases the EMC effect by $\sim 15 \div 20\%$ for ^{4}He and other light nuclei and a factor of two smaller for heavy nuclei.

At the same time as we have already discussed in the case of the heavy nuclei the Coulomb effect contributes to the increase of the EMC effect reducing the hadronic component of the EMC effect. For $A \sim 200$ two effects practically compensate each other (see Fig. 1).

Overall the discussed effects lead to a larger EMC effect for light nuclei and a weaker A-dependence of the hadronic component of the EMC effect for $A \geq 4$.

6 Recent progress in the studies of SRCs in nuclei

Before discussing the A-dependence of the the hadronic EMC effect and its dynamical origin we need to discuss the information about the short-range correlations in nuclei. A very significant progress in this field has been reached in the last few years. As a result it has become possible to perform nearly model independent tests of the role of the SRC in the EMC effect and also strongly constrain the models of the EMC effect.

Hard interactions resolve local structure of the nucleus. Hence they resolve collective low energy scale degrees of freedom (effective interactions) and probe local structure of the nucleus. Since the nuclear forces are short range on the nucleus scale ($r_{NN} < 2fm$) the properties of a nucleon in the nuclear media are determined by its local surrounding. Intuitively it is clear that closer the nucleons get together, the stronger their polarization/deformation is. Hence the configurations where nucleons nearly overlap appear to be a natural candidate for the large hadronic EMC effect. Therefore we need to review briefly the recent progress in the studies of SRCs.

Singular nature of the NN interaction in coordinate space at small inter nucleon distances/large momenta leads to the universal structure of SRCs and to the prediction of the scaling of the ratios of the cross sections of $x > 1$ scattering at sufficiently large $Q^2 \geq 2\text{GeV}^2$ [15]. In particular for $1 + k_F/m_N < x < 2$:

$$R_A(x, Q^2) = \frac{2}{A} \frac{\sigma(eA \to e + X)}{\sigma(e^2H \to e + X)} = a_2(A). \tag{35}$$

Here $a_2(A)$ has the meaning of the relative probability of the two nucleon SRCs per nucleon in a nucleus and in the deuteron, that is, it is the ratio of spectral functions of nucleus to that of deuteron. Actually it includes the contribution of triple nucleon correlation, pn and pp correlations.

The first evidence for such scaling of the ratios was reported in [16]. The extensive studies were performed in [33] using various data taken at SLAC at somewhat different settings which confirmed the scaling of the ratios and for the first time confirmed the prediction [16] of the "super" scaling of the ratios at different Q^2 – the precocious scaling of the ratios plotted as a function of $\alpha_{t.n.}$ – the minimal α for the scattering off two nucleon SRC at rest (the Fermi motion of the pair practically cancels out in such a ratio) [16]:

$$\alpha_{t.n.} = 2 - \frac{q_0 - q_3 + 2m_N}{2m_N}\left(1 + \frac{\sqrt{W^2 - 4m_N^2}}{W}\right), \tag{36}$$

where $W^2 = 4m_N^2 + 4q_0 m_N - Q^2$.

The experiments performed at JLab allowed to explore the scaling of ratios in the same experiment. In [34, 35] the scaling relative to ^{3}He was established. Very recently the results of the extensive study of the nucleus/deuteron ratios were reported in [36] allowing a high precision determination of the relative probability of the two nucleon SRCs in nuclei and the deuteron. The results of [36] are in a good agreement with the early analysis of [33], see Fig. 3.

Several theoretical observations are important for the interpretation of the scaling ratios: (a) The invariant energy of the produced system for the interaction off the deuteron is large on the scale of nuclear phenomena but small as compared to the scale characteristic of hadronic phenomena: $W - m_{2H} \leq 250$ MeV. This kinematics obviously leads to a strong suppression of the production of the inelastic final states. Correspondingly, scattering off exotic configurations which decay into excited baryon states, Δ's, etc is strongly suppressed in the discussed kinematics. (b) The closure is valid for the final state interaction of the nucleons of the SRC and the residual nucleus system. Only the f.s.i. between the nucleons of the SRC contributes to the total (e,e') cross section [33, 6]. Since this interaction is the same for light and heavy nuclei it does not modify the scaling of the ratios. (c) In the limit of large Q^2 and large energy q_0 but the fixed ratio $x = AQ^2/2m_A q_0$, the cross section is expressed through the light - cone projection of the ground state nuclear density matrix, $\rho_A^N(\alpha)$, that is the integral over all components of the interacting nucleon four momentum except $\alpha \equiv p_-/(m_A/A)$, where $p_- = p_0 - (\vec{p}\cdot\vec{q})/|\vec{q}|$. The ratio of the cross sections reaches a plateau at $x(Q^2)$ corresponding to the scattering off a nucleon with minimal momentum $\sim k_F$ indicating that the dominance of two nucleon SRC sets in just above the Fermi surface. (d) Observation of the precocious $\alpha_{t.n.}$ scaling indicates that R_A is equal to the ratio of the light-cone density matrices of the nucleus and deuteron. It also strongly indicates that SRCs of the baryon charge two are predominantly built of two nucleons rather than some exotic states. It is worth noting here that the correspondence between the light cone and nonrelativistic wave functions is pretty straightforward. Hence the results for the ratio of wave functions in the region where pair correlations dominate should be close.

To probe directly the structure of the SRCs it is advantageous to study a decay of SRC after one nucleon of the SRC is removed which is described by the nuclear decay function

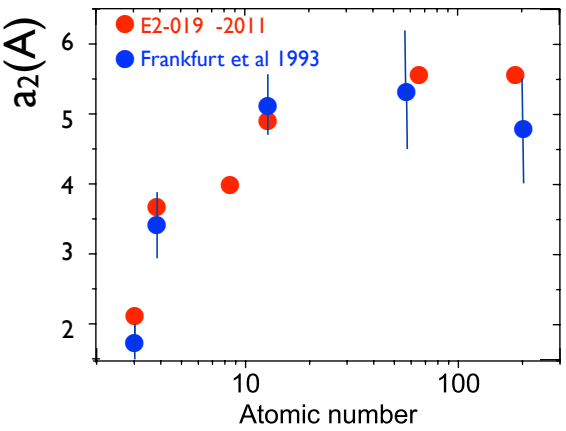

Figure 4: Comparison of the first determination of $a_2(A)$ based on the analysis of the SLAC data [33]with the most recent Jlab measurements [36].

[15, 16]. In the two-nucleon SRC approximation the decay function is simply expressed through the density matrix as the removal of one of the nucleons of the correlation results in the release of the second nucleon with probability of one. A series of the experiments was performed at BNL and JLab which studied (p,2p), (e,e'p) reactions in the kinematics where a fast proton of the nucleus is knocked out (see review and references in [37, 6]). In spite of very different kinematics – removal of forward moving nucleon in the ^{12}C(p,2p) case and backward moving proton in the ^{12}C(e,e'p) case, different probes and different momentum transfer $-t \approx 5$ GeV^2 and $Q^2 = 2$ GeV^2 – the same pattern of the neutron emission was observed: the neutron is emitted with a probability $\sim 90\%$ in the direction approximately opposite to the initial proton direction with the correlation setting in very close to $k_F(C) \sim 220$ MeV/c. The JLab experiment observed in the same kinematics both proton and neutron emission in coincidence with $e'p$ and found the probability of the proton emission to be about 1/9 of the neutron probability. Hence the data confirm our theoretical expectation that removal of a fast nucleon is practically always associated with the emission of the nucleon in the opposite direction with the SRC contribution providing the dominant component of the nuclear WF starting close to the Fermi momentum. The large pn/pp ratio also confirms the standard expectation of the nuclear physics that short-range interactions are much stronger in the isospin zero channel than in the isospin one channel and hence are much more sensitive to the pion-like exchange. Saturation of the probability provides an independent confirmation of the conclusion that at least up to

momenta $\sim 500 \div 600$ MeV/c, SRC predominantly consist of two nucleons.

A word of caution is necessary here. In the standard nuclear physics approach the intermediate Δ isobars play an important role in the $I = 1$ interaction channel. Usually they are absorbed into the definition of the low energy NN potential. However in the case of hard exclusive process the $N\Delta$ SRCs are resolved and may show up and be comparable to pp SRCs.

The structure of SRC depends on x, Q^2 and M^2. Here M^2 is the mass range allowed for the decay of SRC. For M close to $2m_N$ possible exotic states enter into parameters of effective low energy Hamiltonian. With increase of M exotic states may reveal themselves in the decay of SRC. Thus $M-2m_N$ plays the role of the resolution and increasing resolution allows one to investigate some properties of superdense matter which is present in the inner core of neutron stars. Note here that the allowed phase volume was much larger in the BNL A(p,2pn) experiment. So the consistency of two experiments suggests that increase of the resolution does not lead to a drastic change in the structure of the short range nuclear structure.

7 Short-range correlations in nuclei and the A-dependence of the hadronic EMC effect

We will show below that the strength of the deformation of the bound nucleon WF as compared to the free nucleon WF is proportional to its off-shellness. At $x < 0.7$ where the Fermi motion effects are small it is possible to average over nucleon momenta and conclude that the deformation of the structure function of a bound nucleon should be proportional to the nucleon average kinetic energy T_A. Since T_A is dominated by the contribution of the short range correlations [31] in nuclei we can roughly estimate the A-dependence of T_A from the measurements the ratio of the high momentum components in the nuclei and in the deuteron - $a_2(A)$. This ratio is equal to the ratio of the nucleus and the deuteron inclusive (e,e') cross sections in the x region of $1.4 < x < 1.8$ where it exhibits a Q^2 independent plateau - (see discussion in Section 6 and in particular Eq.35).

This information can be used to predict the A-dependence of the hadronic EMC effect for $x = 0.5 \div 0.7$ where nucleon Fermi motion is small for $F_{2N}(x, Q^2) \propto (1 - x)^n, n = 2$ corresponding to the SLAC/Jlab kinematics (cf. Fig.2). Since the Fermi motion is a few % correction which is proportional to the average T_A and most of the kinetic energy originates from the SRCs the overall A-dependence of the hadronic EMC effect including Fermi motion effect should be approximately proportional to $a_2(A) - 1$.

One can see from Figs. 5 that the A-dependence of the "hadronic" EMC effect for $x = 0.5$ is indeed consistent with the A-dependence of $a_2(A) - 1$. It is worth noting here that in [38, 16] it was assumed that **all** $x \geq 0.4$ EMC effect is due to the contribution of the SRCs. (Note here that nucleons belonging to mean field give up to 20% contribution to T_A, leading to a deviation of the A-dependence of T_A and $a_2(A)$.)

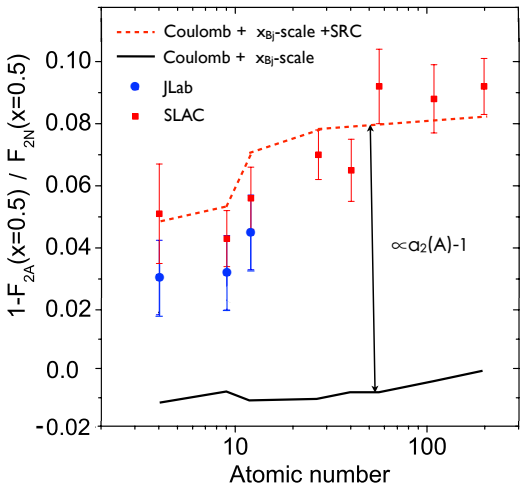

Figure 5: The solid line is the result of calculation taking into account the equivalent photon effect and the effect of proper definition of x. The dashed line is the contribution of the hadronic EMC effect due to SRCs normalized for large A with the A-dependence $\propto a_2(A) - 1$ with $a_2(A)$ from taken from the JLab measurement [36]. The ratio data are from [23, 5].

The data at $x = 0.6$ and $x = 0.7$ where the Fermi motion effect is practically zero for the SLAC kinematics are also consistent with hadronic EMC effect been proportional to $a_2(A) - 1$. To illustrate this proportionality we calculate the difference between the standard model without Fermi motion and the data, which we denote as $\Delta(A)$ and plot it as a function of $a_2(A) - 1$ – Fig. 6. The data are consistent with $\Delta(A) \propto a_2(A) - 1$ though more accurate data would be highly desirable.

To analyze the A-dependence of the hadronic EMC effect at $x > 0.5$ we need to take into account the nucleon Fermi motion effect which rapidly increases with x for $x \geq 0.55$ and which is $\propto T_A$ in the discussed x-range (Eq.17) and results including Fermi motion – dashed curves in Fig. 2a, 2b). One can see that the difference between dashed curves and the data is much larger than the difference between the standard model without Fermi motion and the data already for x=0.6. This implies right away that the hadronic EMC effect is roughly $\propto T_A$. To check it with a better accuracy we can focus on the A-dependence of the difference between the standard model without Fermi motion and the data, which we denote as $\Delta(A)$. In Fig. 6 it is plotted as a function of $a_2(A) - 1$. The data are consistent with $\Delta(A) \propto a_2(A) - 1$ though more accurate data would be highly desirable. Thus we conclude that in the range: $0.5 \leq x \leq 0.7$ the hadronic EMC effect is approximately proportional to the probability of two nucleon correlations in nuclei or practically equivalently to the average nucleon kinetic energy of nucleon in nucleus.

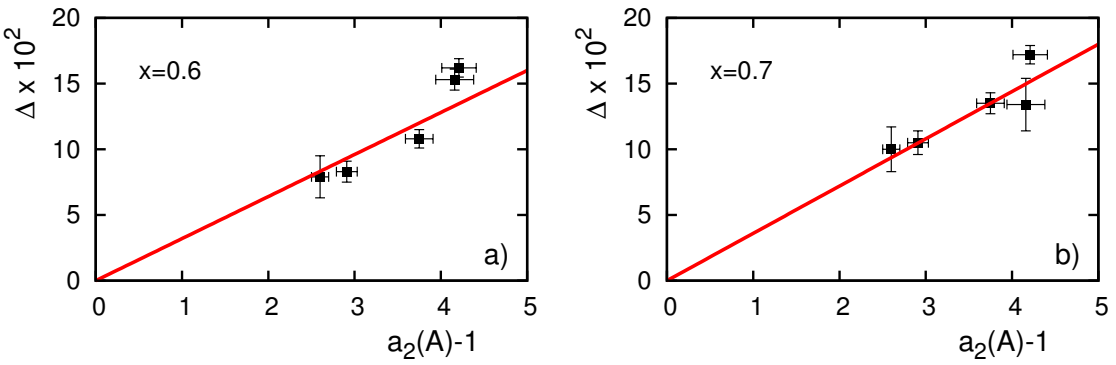

Figure 6: A-dependence of the hadronic EMC effect for $x = 0.6$ and $x = 0.7$. The data are from [23].

For larger x this pattern should break down since the expansion in powers of (1-x) breaks down. In fact for $x \sim 1$ we expect $F_{2A}/F_{2\,^2H} \propto a_2(A)$ rather than $F_{2A}/F_{2\,^2H} - 1 \propto a_2(A)$.

Theoretical and phenomenological arguments in favor of the similarity of the A-dependence of the EMC effect and the two nucleon SRCs were first presented in [19, 16] for $x \geq 0.5$. New data on the A-dependence of SRCs allowed to demonstrate proportionality of the EMC effect to the probability of the two nucleon correlations in nuclei without employing model for the A-dependence of SRCs [39]. The authors assumed that the SRCs dominate the EMC effect for the $R_A(x_p)$ ratio for all x. They focused on the x-slope of the ratio in the $x = 0.35 - 0.7$ range which is less sensitive to the absolute normalization of the data assuming that the data can be fitted as a linear function of x. As we have seen above accounting for the standard model effects (which in most of the range studied in [39] constitutes less than 20% of the difference of $R_A(x_p)$ from unity) does not change this conclusion qualitatively. Still it may suggest that the A-dependence of the hadronic component of the EMC effect between $A = 4$ and $A = 200$ is somewhat stronger than given purely by SRCs.

As we discussed already in section 3 the Fermi motion effect is very different for moderate and large Q^2. Assuming that the hadronic EMC effect can be described by the deformation of the bound nucleon wave function which is to the first approximation proportional to T_A we can estimate deviation of $R_b(x, Q^2) = F_{2N}^{bound}(x, Q^2)/F_{2N}^{free}(x, Q^2)$ from unity assuming factorization of the correction to the EMC ratio as a product of the nucleon modification effect and the Fermi motion and correcting for the x-scale and Coulomb effects. For $n = 2$ and $x > 0.7$ ($n = 3$ and $x > 0.6$ this procedure breaks down since in the convolution larger than average nucleon momenta contribute leading to overestimate of $1 - R_b(x, Q^2)$ for such x. A separate analysis is required for this kinematics which will be presented elsewhere.

The estimate of $1 - R_b(x, Q^2)$ is presented in Fig. 7 based on the analysis of the SLAC

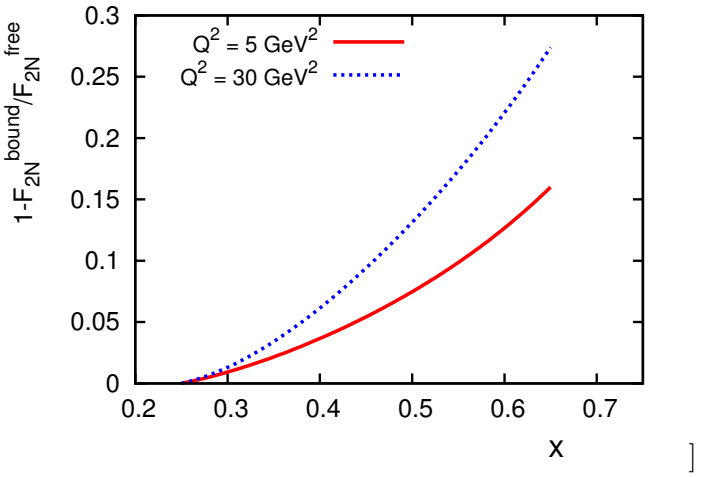

Figure 7: Estimate of the ratio of the bound and free nucleon structure functions in medium and heavy nuclei as a function of x.

data[23] for moderate Q^2 and BCDMS [24] and NMC [25] data for large Q^2.

We see that deformation rapidly grows with increase of x starting at $x \sim 0.5$. There is a trend for the higher Q^2 data to indicate a stronger deformation of the bound nucleon wave function which may indicate a difference in the leading and higher twist effects in the interaction with the bound nucleon. However the errors of the high Q^2 data are very large for $x \geq 0.55$, see Fig. 2.

Since the bound nucleon deformation effect is small up to $x \sim 0.5$ and the probability of having a quark in a nucleon with $x > 0.5$ is $\sim 2 \cdot 10^{-2}$ we conclude that the EMC effect probes very rare deformations of bound nucleons. The deviations from the discussed approximation on the level of $2 - -3\%$ at $x \sim 0.2 \div 0.4$ cannot be excluded experimentally so one can only conclude that the accuracy of the approximation where nucleus consists of nucleons whose structure function coincides with that for free ones (+ equivalent photons) is on the level of few % for $x \leq 0.5$ where the contribution of the mean field approximation to the nucleus WF dominates.

Our analysis also allows to put an upper limit

$$\eta_\pi(A \sim 200) \leq 5.0\%. \tag{37}$$

on the fraction of energy carried by pion constituents of nuclei assuming that all deviation of $R_A(x \sim 0.6, Q^2 \sim 5\text{GeV}^2)$ from the standard model is due to the pion field.

8 Constraints on the models of the EMC effect

In this section we briefly summarize the constraints on the possible mechanism of the hadronic EMC effect and confront different classes of models of the EMC effect with these constraints. Majority of models ignore the effects described by the standard model and hence should be modified to account for the QCD dynamics to describe data. So we restrict our discussion by consideration of constraints on the basic features of these models. The most important of these constraints are obtained from the following:

- Additivity of nucleon structure functions as a function of Bjorken x follows from QCD dynamics of hard processes and parton structure of nucleons and nuclei to the extent that non-nucleonic degrees of freedom can be ignore leading to $R_A(x, Q^2)$ close to one.
- Probability conservation: the baryon and momentum sum rules.
- Difference between the fraction of nucleus momentum and nucleon carried by equivalent photons is accurately calculated in QED.
- The hadronic EMC effect is small for $x < 0.5$ and for larger x rapidly increases with increasing x, see Fig. 7.
- The A-dependence of the hadronic EMC effect is rather close to the A-dependence of the the short-range internucleon correlations, cf. discussion in section 7.
- High probability of short-range correlations $\sim 20 \div 25\%$ and dominance of the nucleonic degrees of freedom ($> 80\%$) in the correlations, cf. brief review of existing data in section 6.
- No enhancement of the antiquark distribution in nuclei is present for $x \sim 0.1$ with accuracy $\approx 1\%$ [3].
- Q^2-dependence of the magnetic form factor of bound nucleons with small momenta is very close to that of free nucleons [40].

Seemingly natural treatment of the EMC effect within the standard nuclear physics approaches is to explicitly include mesonic degrees of freedom in the nuclear wave function. Pions with small momenta $\approx m_\pi$ relevant for the Chiral QCD Lagrangian give insignificant contribution into antiquark distribution at $x \geq 0.2$. However a significant enhancement of the pion field of nuclei at large pion momenta as compared to the system of free nucleons was found for example in [41]. Within the nonrelativistic nuclear theory where inner motion is unrelated to the c.m. motion this prediction may be translated into light cone dynamics where the fraction of nucleus momentum (scaled by 1/A) carried by a pion is given by the formulae: k_3/m_N where k_3 is the projection of pion momentum on the direction supplied by

photon momentum. Prediction of the enhancement of pion field at large pion momenta is in variance with the lack of modification of the antiquark distribution in the nuclei observed in the measurement of the Drell Yan pairs [3]. To fit the data on the EMC effect authors need to assume that mesons carry $\eta_\pi \sim 4\%$ fraction of the nucleus light cone momentum which is hardly consistent with experimental restrictions on antiquark distribution in nuclei. The models which describe nucleus wave function by a vertex function with interacting nucleon off mass shell and the residual system on mass shell, are effectively in the same category as they have to compensate the violation of the momentum sum rule by introducing an additional (presumably mesonic) component in the nucleus wave function. These models typically predict an enhancement of the antiquark $\bar{u} + \bar{d}$ distribution in nuclei of the order of 10–20% at $x \sim 0.1$, while according to the data [3] $\bar{q}_A/\bar{q}_N \leq 1$ for this x-range (the absolute accuracy of these measurements is of the order of 1%).

Another class of nuclear models is mean field models where a nucleon is treated as moving in the self consistent field of other nucleons with a deformation of a bound nucleon (nucleon swelling, ...) independent from nucleon momentum (for a review and references see [42]). These models ignore the experimental observation of SRCs in nuclei, and they do not provide an explanation for the similarity of the A-dependence of the hadronic EMC effect to the A-dependence of the two nucleon SRCs. The similarity of the Q^2-dependence of the nucleon magnetic form factors of the low momentum bound nucleons to that of the free nucleons is not reconciled in these models with the large hadronic EMC effect. The fast onset of the hadronic EMC effect with x for $x > 0.5$ and lack of the significant effect at smaller x were not predicted in these models.

In a number of models it was assumed that nonnucleonic configurations – six quark configurations, Δ isobars, etc – are present in nuclei with significant probability. If the SRCs were an *incoherent* superposition of nucleonic and non-nucleonic configurations one would not be able to generate an EMC effect larger than 20% of the probability of the SRCs, which is $\leq 5\%$. This is clearly insufficient to explain the strength of the EMC effect of the order of 15% for $x \geq 0.6$ and $A \geq 40$. If one would assume that there exist both nucleonic SRC and exotic configurations with a probability $\geq 20\%$, necessary to fit the EMC effect, the number of nucleons below the Fermi surface would drop below 60% which is hardly consistent with the current experience of the nuclear physics.

To summarize, the common perception that there exist plenty of successful models of the EMC effect mostly arises from treating the EMC effect as an isolated phenomenon ignoring the totality of the constraints which were obtained from the studies of the hard nuclear phenomena in the past 20 years. At the moment there seems to be no viable alternative to the scenarios where the EMC effect is associated with modifications of rare quark-gluon configurations selected by hard probe, and which become larger with increase of the bound nucleon momentum.

9 How nuclear medium modifies nucleon breathing

9.1 Deformations of bound nucleon wave function within QCD

A solution proposed in [38] is the mechanism where hard scattering off quarks selects at $x \geq 0.5$ rare quark-gluon configurations in bound nucleons and that the deformation of the bound nucleon WF is enhanced for such rare configurations. The mechanism is based on two fundamental and well established properties of QCD.

Any characteristics of a composite system should fluctuate and depend on the process. The textbook example in QED (the abelian gauge theory) is the hydrogen atom where the calculation of moments of the hydrogen radius finds that $\langle < r^n \rangle = \int d^3 r r^n \psi^2(r)$ differs from $\langle r \rangle^n$. An example of observed fluctuations in QCD is the significant difference between the electric and axial radii of the proton: $\langle r^2_{e.m.} \rangle^{1/2}$ =0.85 fm, $\langle r^2_{axial} \rangle^{1/2} \approx 0.65$ fm. The fluctuations of strength of interaction also play a key role in the explanation of the phenomenon of high energy inelastic diffraction. One can prove that in QCD as in QED interaction of a hadron in a small size configuration with a hadron target is much weaker than in an average configuration.

Two patterns of fluctuations of interactions are well understood in QCD. One type of fluctuations arises as the consequence of the dependence of interaction on the spatial size of color neutral configuration. This pattern is observed in particular in the color transparency phenomenon, for the recent review see

reveals in pion-nucleus interaction in the form of color transparency phenomenon in coherent production of two jets , cf.review and corresponding references in [43].

Another pattern of fluctuations of strengths of interaction follows from the dependence of interaction on the representation of color group of $SU_c(3)$ characterizing constituents in color space. This property is well known in respect to the invariant charge as the dependence of Casimir operators of color group $SU_c(3)$ on representation:the ratio of Casimir operators for octet and triplet representations: $F^2(8)/F^2(3) = 9/4$. These fluctuations are important for hard processes which we discuss in the next subsection. In the low energy processes instant interaction is averaged out and cannot reveal itself. On the contrary it follows from the QCD factorization theorem that a hard probe selects particular instantaneous quark-gluon configuration in a hadron target. Another feature of QCD is that the number of constituents is decreasing with decrease of the overall size. (Last property reveals itself in the x dependences of parton distributions, in the special high energy processes, etc.)

Difference in the fluctuations of the wave function of a bound and free nucleon leads to the deformation of its wave function. This phenomenon is well known in atomic physics from the application of the variational principle to the hydrogen molecule, H_2. At large inter proton distances the main effect is swelling of the hydrogen WFs while at small interproton distances the overall size of the hydrogen atoms is reduced [44].

The use of the variational principle allows us to understand the qualitative trend in

QCD as well – probabilities of the quark-gluon configurations within a bound nucleon for which attraction is weaker than in average, should be reduced, while probabilities of configurations for which attraction is stronger than in average should be enhanced. (This is a particular case of the application of the Le Chatelier's principle.)

In [16] the expressions were derived for the reduction of the probability of the configurations in bound nucleons which interact with strength much smaller than average:

$$\langle\delta\rangle = 1 + \frac{4\langle U\rangle}{\Delta E}, \tag{38}$$

where $\langle U\rangle$ is the expectation value of the potential acting on a nucleon in the nucleus, $\Delta E = M_{N^*} - M_N \sim 400 \div 600 MeV$ is characteristic energy of excitation of the nucleon. Hence for a heavy nucleus a maximal suppression is of the order 20%. The calculation of the suppression effect for the case of quark-gluon configurations for which strength of interaction is smaller but still comparable to $\langle U\rangle$ requires use of a specific model, see [45].

One can use equations of motion to derive the dependence of the suppression on the momentum of the bound nucleon [38]. In the lowest order in $k^2/m_N\Delta E$ neglecting term $\propto \epsilon_A/\Delta E$ one finds

$$\delta(k) = 1 - 2k^2/m_N\Delta E. \tag{39}$$

Eq.39 including the binding term can be written in a compact form if one substitutes k^2 in Eq.39 by

$$\Delta m^2 = m_N^2 - (p_A - p_{rec})^2. \tag{40}$$

where p_{rec} is the four momentum of the A-1 nucleon recoil system in the process where a nucleon was removed from the nucleus. The possibility to rewrite Eq.38 in this form was first pointed out in [46]. A detailed analysis which demonstrated validity of the formula for the case of generic final state of the nucleus was performed in [31]. Note here that Eq.39 naturally satisfies the requirement that the scattering amplitude when continued to the pole where $\Delta m^2 = 0$, should coincide with the on-shell amplitude. Hence the linear dependence on off-shellness for small Δm^2 should be valid for wide range of bound nucleon deformation effects. In particular such a pattern is consistent with the measurements of the deviation of the ratio G_E^{bound}/G_M^{bound} from the free value which was studied in the JLab experiment [47].

9.2 Implications for nuclear pdfs at large x

The studies of the x-dependence of nucleon pdfs find a very different dependences on large x: $xV_N(x,Q^2) \propto (1-x)^3$, $x\bar{q}_N(x,Q^2) \propto (1-x)^7$ and $xG_N(x,Q^2) \propto (1-x)^5$. This dependence indicates that hard interaction with nucleon at $x \geq 0.6$ selects quark - gluon configurations in which antiquarks in the nucleon and in particular the meson field is suppressed. The suppression of the interaction of nucleons in such configurations can be demonstrated in the perturbative QCD and on the level of emission of mesons as suppression of the pion emission by a small size configurations in a nucleon (see analysis in Appendix D of [16]).

At the same time the analyses of low energy nucleon - nucleon interaction suggest that the dominant contribution to the SRC for $k \leq 600$ MeV/c originates from the $I = 0, S = 1$ channel where pion exchange plays a very important role (see e.g. [48]).

Combining this observation with the arguments of the previous subsection we conclude that probability of configurations with large x partons should be suppressed in the bound nucleons with the amount of the suppression comparable to the one given by Eq.38 which is of correct magnitude to explain the EMC effect for $x \sim 0.6 \div 0.7$.

In the limit when one can average over the Fermi motion of nucleons ($x \leq 0.6$) we find for the A-dependence of $\langle\delta\rangle$:

$$1 - \langle\delta\rangle = \langle 2k^2/\Delta E\rangle \propto T_A/m_N \propto a_2(A) \tag{41}$$

Hence we conclude that for the discussed kinematics the hadronic EMC effect should be proportional to $a_2(A)$ with a good accuracy which is indeed the case, see the discussion in section 6.

9.3 Zooming on the nucleon polarization

The critical test of the discussed picture would be a study of the dependence of the nucleon deformation on the nucleon momentum which for a large range of nucleon momenta should be proportional to the square of the momentum of the struck nucleon.

The key experiment to test the discussed interpretation would be a measurement of the tagged EMC effect [38], the process $e +^2 H \to e + N + X$ with detection of the recoil nucleon with light cone fraction $\alpha > 1$. In this process one can measure the bound nucleon structure function $F_{2N}^{bound}(x/\alpha)$. We expect that

$$1 - F_{2N}^{bound}(x/\alpha, Q^2)/F_{2N}(x/\alpha, Q^2) = f(x/\alpha, Q^2)\delta m^2, \tag{42}$$

with $f(x/\alpha, Q^2)$ small for $x/\alpha < 0.5$ and rapidly growing at larger x/α. A fast dependence of the effect on x/α would make it easier to separate it from possible final state interaction effects [6].

A priori the deformation of a bound nucleon can also depend on the angle ϕ between the momentum of the struck nucleon and the reaction axis as

$$\frac{\frac{d\sigma}{d\Omega}}{\langle\frac{d\sigma}{d\Omega}\rangle} = 1 + c(k, q). \tag{43}$$

Here $\langle\sigma\rangle$ is cross section averaged over ϕ and $d\Omega$ is the phase volume and the factor c characterizes non-spherical deformation. Correlation between the photon polarization and $\vec{k}$ direction is also possible.

[6] In the case of the experiments planned at Jlab one would have to address the issue of the role of the higher twist effects for $F_{2N}(x \sim 0.5, Q^2)$.

Such non-spherical polarization is well known in atomic physics. Contrary to QED detailed calculations of this effect are not possible in QCD. However, a qualitatively similar deformation of the bound nucleons should arise in QCD. One may expect that the deformation of bound nucleon should be maximal in the direction of radius vector between two nucleons of SRC. [7] The ϕ-dependent shape deformations of bound nucleons are averaged out in the EMC effect for $x < 0.7$.

As we mentioned above a non-spherical nucleon deformation may be manifested in the polarization effect in the process $\vec{e}+^4He \to e+\vec{p}+^3H$ where the the measured asymmetry can be interpreted in terms of the deviation of ratio G_E/G_M for a bound nucleon from the free value. It would be interesting to check whether the same pattern is observed for the scattering off the deuteron, whether the linear dependence on Δm^2 extends up to larger nucleon momenta and look for the dependence of the effect on the angle ϕ. Since the deformation is expected to be strongest along the radius vector between the nucleons, one may expect the deviations from the free nucleon case to be maximal for $\phi \sim 0, \pi$.

10 Conclusions

Application of the baryon charge and momentum QCD sum rules allows us to prove that the EMC effect is a genuine nuclear effect. To extract hadronic EMC effect from data one should take into account the model independent effects. Additivity of the nucleus structure functions follows from nuclear physics ideas if the Bjorken x is used for the scattering off nuclei as dictated by the parton model and QCD. Account of QED requires to include the equivalent photon component of the light-cone WF of the heavy nucleus. Comparison of nuclear and deuteron structure functions at the same variable x_p leads to underestimate of the EMC effect for for all nuclei. At the same time the two effects we discussed mostly compensate each other in the case of hadronic component of the EMC effect for heavy nuclei.

The data indicate that the hadronic EMC effect is a predominantly a high x phenomenon. The A-dependence of the hadronic EMC effect is consistent with the A-dependence of the two nucleon correlations. The implementation of above mentioned effects impacts also on the nucleon pdfs extracted from the data and in particular somewhat increases the nuclear correction for extraction of $F_{2n}(x, Q^2)$ from the deuteron data.

We also emphasized that the presence of predominantly nucleonic SRC in nuclei together with the similar A-dependence of SRCs and the hadronic EMC effect, and lack of the nuclear enhancement of antiquark distribution in nuclei, put strong constraints on the mechanism of the EMC effect. These data pose a serious problem for the mean field models where SRC are absent. At the same time they are consistent with the scenario of the nucleon deformation occurring predominantly due to suppression of small size, large

[7] We are indebted to H. Bethe(1995) and V.Gribov(1993) who draw attention of one of us (MS) to this effect.

x configurations in the bound nucleons. It is based on the well established properties of bound states in QCD: presence of fluctuations with strength of the interaction and of quark-gluon content, and selection of the certain instantaneous quark-gluon configurations by hard processes. Deformation of peripheral pion cloud of a nucleon is suppressed since in low energy QCD pion-pion interaction is suppressed by high power of pion momentum.

It is important to perform further experimental measurements of the EMC ratio for $x \geq 0.5$ at large Q^2 which will become feasible at JLab 12. Especially interesting would be to study the ratio of the EMC effect in ^{48}Ca and ^{40}Ca since in this case the standard model leads to the same nuclear effect. Moreover such research would provide a unique window on the structure of neutron rich high density nuclear matter relevant for description of the cores of the neutron stars.

The critical tests of the current ideas will be possible in the processes where momentum of the struck nucleon is tagged. It is expected that effect should be proportional to the nucleon off-shellness and may also depend on the direction between the momentum of the struck nucleon and the virtual photon momentum (polarization).

It would also be interesting to analyze the role of the violation of the isotopic invariance due to presence of the Coulomb field in nuclei and in particular the difference of the momentum fraction carried by photons in protons and neutrons ($\eta_\gamma(p) - \eta_\gamma(n) \approx 0.2\%$) and its role in the extraction the Weinberg angle from neutrino data[49].

Acknowledgements

We thank W.Vogelsang for informing us about early studies of the effect of the Coulomb field in nucleons. We are indebted to V.Gribov(1993) and H.Bethe (1995) who draw our attention to angular asymmetry of deformation of atoms in QED in the close interaction. We also thank C. Ciofi degli Atti and L. Kaptari for the collaboration studies of the color fluctuation model. We thank V. Guzey for pointing out the sign error in the original reconstruction of $R_A(x, Q^2)$ from experimental data presented as a function of x_p and help with generating several plots. We thank Or Hen for discussion of the x-dependence of F_{2N} in the kinematics of the JLab and SLAC experiments. The research was supported by DOE and BSF.

References

[1] EM Collab., J. J. Aubert et al., Phys. Lett. **B 123**,275 (1983).

[2] R. G. Arnold et al., Phys. Rev. Lett. **52** 1431 (1984).

[3] D. M. Alde, H. W. Baer, T. A. Carey, G. T. Garvey, A. Klein, C. Lee, M. J. Leitch and J. W. Lillberg *et al.*, Phys. Rev. Lett. **64**, 2479 (1990).

[4] M. Arneodo, Phys. Rept. **240**, 301 (1994).

[5] J. Seely *et al.*, Phys. Rev. Lett. **103**, 202301 (2009) [arXiv:0904.4448 [nucl-ex]].

[6] L. Frankfurt, M. Sargsian, M. Strikman, *Int. J. Mod. Phys.* **A23**, 2991-3055 (2008). [arXiv:0806.4412 [nucl-th]].

[7] J. Arrington, D. W. Higinbotham, G. Rosner and M. Sargsian, arXiv:1104.1196 [nucl-ex].

[8] L. Frankfurt, V. Guzey and M. Strikman, Phys.Rep. **512**, 255-393 (2012), arXiv:1106.2091 [hep-ph].

[9] L. Frankfurt, M. Strikman, Phys. Rev. **C82**, 065203 (2010). [arXiv:1009.4920 [nucl-th].

[10] E. Fermi, Z. Phys. **29**, 315 (1924);

C. F. von Weizsacker, Z. Phys. **88**, 612 (1934).

E. J. Williams, Phys. Rev. **45**, 729 (1934).

[11] B.A. Kniehl, Phys. Lett. B254 (1991) 267.

[12] M. Gluck, M. Stratmann and W. Vogelsang, Phys. Lett. B **343**, 399 (1995).

[13] M. Gluck, C. Pisano and E. Reya, Phys. Lett. B **540**, 75 (2002) [arXiv:hep-ph/0206126].

[14] H. Honkanen, M. Strikman and V. Guzey, arXiv:1310.5879 [hep-ph].

[15] L. L. Frankfurt, M. I. Strikman, *Phys. Rept.* **76**, 215-347 (1981).

[16] L. L.Frankfurt and M. Strikman, Phys. Rep. **160** (1988) 235-427.

[17] S. V. Akulinichev, S. A. Kulagin and G. M. Vagradov, Phys. Lett. B **158**, 485 (1985); S. V. Akulinichev, S. Shlomo, S. A. Kulagin and G. M. Vagradov, Phys. Rev. Lett. **55**, 2239 (1985).

[18] B. L. Birbrair, A. B. Gridnev, M. B. Zhalov, E. M. Levin and V. E. Starodubsky, Phys. Lett. B **166**, 119 (1986).

[19] L. L. Frankfurt and M. I. Strikman, Phys. Lett. B **183**, 254 (1987).

[20] G. B. West, Phys. Lett. B **37**, 509 (1971).

[21] P.Bosted, https://userweb.jlab.org/ bosted/fits.html;

L. W. Whitlow, E. M. Riordan, S. Dasu, S. Rock and A. Bodek, Phys. Lett. B **282**, 475 (1992).

[22] A. C. Benvenuti *et al.* [BCDMS Collaboration], Phys. Lett. B **223**, 485 (1989).

[23] J. Gomez *et al.*, Phys. Rev. D **49**, 4348 (1994).

[24] A. C. Benvenuti *et al.* [BCDMS Collaboration], Phys. Lett. B **189**, 483 (1987).

[25] P. Amaudruz *et al.* [New Muon Collaboration], Z. Phys. C **53**, 73 (1992).

[26] K. Hencken *et al.*, Phys. Rept. **458**, 1 (2008) [arXiv:0706.3356 [nucl-ex]].

[27] G. Sterman, An introduction to QUANTUM FIELD THEORY Cambridge, University Press, 1993.

[28] V. N. Gribov, "The theory of complex angular momenta: Gribov lectures on theoretical physics," *Cambridge, UK: Univ. Pr. (2003) 297 p*

[29] L. Frankfurt, G. A. Miller and M. Strikman, Phys. Rev. D **65**, 094015 (2002) [arXiv:hep-ph/0010297].

[30] I. Angeli, Atomic Data and Nuclear Data Tables, **87**, 185 (2004).

[31] C. Ciofi degli Atti, L. L. Frankfurt, L. P. Kaptari and M. I. Strikman, Phys. Rev. C **76**, 055206 (2007) [arXiv:0706.2937 [nucl-th]].

[32] A. Daniel, J. Arrington, D. Gaskell, AIP Conf. Proc. **1369**, 98-105 (2011). [arXiv:1101.2651 [nucl-ex]].

[33] L. L. Frankfurt, M. I. Strikman, D. B. Day, M. Sargsian, *Phys. Rev.* **C48**, 2451-2461 (1993).

[34] K. S. Egiyan *et al.* [CLAS Collaboration], *Phys. Rev.* **C68**, 014313 (2003). [nucl-ex/0301008].

[35] K. S. Egiyan *et al.* [CLAS Collaboration], *Phys. Rev. Lett.* **96**, 082501 (2006).

[36] N. Fomin, J. Arrington, R. Asaturyan, F. Benmokhtar, W. Boeglin, P. Bosted, A. Bruell, M. H. S. Bukhari *et al.*, [arXiv:1107.3583 [nucl-ex]].

[37] R. Subedi, R. Shneor, P. Monaghan, B. D. Anderson, K. Aniol, J. Annand, J. Arrington, H. Benaoum *et al.*, *Science* **320**, 1476-1478 (2008). [arXiv:0908.1514 [nucl-ex]].

[38] L. L. Frankfurt, M. I. Strikman, Nucl. Phys. **B250**, 143-176 (1985).

[39] L. B. Weinstein, E. Piasetzky, D. W. Higinbotham, J. Gomez, O. Hen, R. Shneor, Phys. Rev. Lett. **106**, 052301 (2011). [arXiv:1009.5666 [hep-ph]].

[40] I. Sick, Phys. Lett. **B157**, 13 (1985).

[41] B. L. Friman, V. R. Pandharipande and R. B. Wiringa, Phys. Rev. Lett. **51**, 763 (1983).

[42] I. C. Cloet, W. Bentz and A. W. Thomas, AIP Conf. Proc. **1261**, 92 (2010).

[43] D. Dutta, K. Hafidi and M. Strikman, Prog. Part. Nucl. Phys. **69**, 1 (2013) [arXiv:1211.2826 [nucl-th]].

[44] J. C. Slater, Quantum theory of Molcules and Solids, v.1, McGraw-Hill Book Company, inc, 1963.

[45] M. R. Frank, B. K. Jennings and G. A. Miller, Phys. Rev. C **54**, 920 (1996) [nucl-th/9509030].

[46] W. Melnitchouk, M. Sargsian and M. I. Strikman, Z. Phys. A **359**, 99 (1997) [nucl-th/9609048].

[47] S. P. Malace, M. Paolone, S. Strauch, I. Albayrak, J. Arrington, B. L. Berman, E. J. Brash and B. Briscoe *et al.*, Phys. Rev. Lett. **106**, 052501 (2011) [arXiv:1011.4483 [nucl-ex]].

[48] N. Kaiser, S. Gerstendorfer and W. Weise, Nucl. Phys. A **637**, 395 (1998) [nucl-th/9802071].

[49] K. S. McFarland [NuTeV Collaboration], AIP Conf. Proc. **655**, 68 (2003).